Numerical and Experimental Performance Investigation of Vertical-Axis Hydrokinetic Turbine

Muluken Temesgen Tigabu[1,3](✉), D. H. Wood[2], and Bimrew Tamrat Admasu[3]

[1] BahirDar Energy Center, BahirDar Institute of Technology, BahirDar University, P.O.BOX 26, Bahir Dar, Ethiopia
[2] Department of Mechanical and Manufacturing Engineering, University of Calgary, Calgary, AB T2N 1N4, Canada
[3] Faculty of Mechanical and Industrial Engineering, BahirDar Institute of Technology, BahirDar University, Bahir Dar, Ethiopia

Abstract. We presented the performance of H-type vertical axis hydrokinetic turbine (VAHKTs). To study the hydrodynamics of VAHKTs an analytical method using a double multi-stream tube (DMST) model was used and an experimental study was employed to validate the DMST results. The key difficulty in the development of VAHKTs technologies is the limited number of researches that show the actual performance under different water velocities. We developed a Matlab code to predict the performance and for validation experimental investigations were performed. The performance operational parameters of power coefficient (C_P) and torque coefficient (C_Q) were used with tips speed ratio (TSR). To validate the DMST and experimental results we used a reference turbine (RM2) developed by the USA Department of Energy's (DOE). A good agreement was found between the analytical and experimental results with the reference turbine. From the study, it is found that the C_P of VAHKTs show an increment and then decrease as the TSR increased. The operating region for VAHKTs is between $1.2 \leq TSR \leq 3.8$. The study illustrated that at $TSR \geq 4$ it is found that there is no power generation from VAHKTs. As s result, the Matlab code we developed based on DMST can be used as a cost effect and robust tool to design and predict the performance of VAHKTs.

Keywords: DMST model · RM2 reference turbine · Hydrodynamics performance · Power coefficient · VAHKTs

1 Introduction

Hydropower conversion is the use of energy contained in the flowing water into the mechanical rotation. It has been used to run wheels for grinding grain in ancient times and to generate electricity in modern times.

M. L. Berihun (Ed.): ICAST 2021, LNICST 412, pp. 506–521, 2022.
https://doi.org/10.1007/978-3-030-93712-6_34

A	Swept area m^2	N	Number of blades (-)
a_{up}	Upwind induction factor (-)	N_h	Number of stream tubes (-)
a_{dn}	Downwind induction factor (-)	Q	Torque (N.m)
c	Blade chord (m)	R	Rotor radius (m)
C_D	Drag coefficient (-)	Re	Reynolds number (-)
C_L	Lift coefficient (-)	V_{up}	Upstream velocity (m/s)
C_N	Normal force coefficients (-)	V_{dn}	Downstream velocity (m/s)
C_T	Tangential force coefficient (-)	V_e	Equilibrium velocity (m/s)
C_q	Torque coefficient (-)	V_∞	Free wind velocity (m/s)
C_P	Power coefficient (-)	W	Relative velocity (m/s)
F_N	Normal force component (N)	α	angle of attack
F_T	Tangential force component (N)	θ	azimuth angle

According to the International Renewable Energy Agency (IRENA) today, hydropower is among the most cost-effective means of generating electricity with a total installed capacity of 1308 GW worldwide and 3817 MW for Ethiopia in 2019. The basic principle of hydropower energy conversion is the use of water to drive the turbines. The energy contained in the water can be used to drive the turbine in two different ways, (1) by use of large reservoirs such as dams to store water and the stored water potential energy used to drive the turbine and (2) without dams and reservoirs, only the kinetic energy of the water is used to drive the turbine. However, recent criticisms have been raised against dam-based hydropower plants (for example, [19,20,25]) due to their versatile effect on the ecosystem, land use, and aquatic life. According to the status report of International Hydropower Association [2] the five years between 2015–2019, the growth in installed capacity was limited 2.1% and 1.2% in 2019.

On the other hand without dam hydropower plant has got considerable attention as an environmentally-friendly option due to smaller effect on the ecosystem. A key aspect of without dam hydropower is producing power at a smaller scale, the frequent term to describe such technologies is hydrokinetic turbines (HKTs). HKTs is a collective term used to refer to the energy generated from the moving water of the currents in oceans, tidal, rivers, and human-made water structures. HKT technologies can be categorized into two main groups by M. Anyi and B. Kirke [1], (1) the axial flow turbine and (2) the cross-flow turbine (other kinds of literature also used vertical axis). There are two types of cross-flow turbine – also called vertical axis turbines: The Savonius type (based on the drag force) and the Darrieus type turbines (based on the lift force). Furthermore, the Darrieus type can also be classified based on the type of rotor as helical or straight (H-type). A detailed review on the classification of HKTs is provided by [13], this paper will focus on H-type Darrieus Vertical axis hydrokinetic turbine (VAHKTs).

The merits of generating electricity using VAHKTs include simple structural components, independence to water current direction, generating power from any direction of the current, no need for a yaw mechanism, and easier maintenance. The working principle and design Methodology of HKTs are similar to the wind energy conversion system. For an equal cross-sectional area, a wind speed of 10 m/s has the same incoming kinetic power as a water flow speed of 1.1 m/s and in general, VAHKTs can be installed in a flow of water velocity starting from 0.5 m/s and above [8]. However, the wind energy sector is matured and at a fully commercialized stage while HKTs still in a developmental phase and have not been fully commercialized yet, due to their reliability and low power density [6]. The study of HKTs is a growing field of renewable energy research, and it can make a big difference to power communities in remote locations [23].

Due to poor conversion efficiency, the performance investigation of VAHKTs has received considerable critical attention such as [9,22,23]. However, most of the studies have been carried out and available in the open literature on the performance investigation of vertical axis wind turbines, experimental by [24, 26] Analytical parametric performance investigation by [4,14,17]. For VAHKTs limited studies are available on the actual performance of VAHKTs (for example, [12] presented the design consideration and performance of VAHKTs for river applications). However, the research efforts in HKTs technology are rather scarce and the knowledge base is quite deficient. Therefore, this study makes a major contribution to research on VAHKTs by investigating the actual performance.

The hydrodynamics of VAHKTs is quite complex due to variation in the local angle of attack, local relative flow velocity, tangential, and normal forces [8]. Several mathematical models have been developed to investigate the performance of VAHKTs, a detailed compressive review of these models is given by [7,11]. Under the current investigation, this paper used the double multi-stream tube model (DMST) which was first introduced by Paraschivoiu [16].

This paper aims to investigate the performance of VAHKTs using Analytical and experimental methodologies. A Matlab code based on DMST is used to predict the performance and further experimental results were used to validate the analytical method. The importance and originality of this study are that it explores the actual performance of VAHKTs and develops a cost effect prediction model for fast implementation and design. The findings should make an important contribution to the applicability of VAHKTs for remote regions in off-grid areas where the operating cost of fuel-based power generation is high.

2 Materials and Methods

2.1 Mathematical Formulation of the Hydrodynamics Model

The design methodology for VAHKTs shares similar principles with the vertical axis wind turbine. The philosophy applied to the study of vertical axis wind turbines is aerodynamics whereas for VAHKTs similar hydrodynamic models can be used. The total power generated from HKTs is determined in a similar fashion with that of wind energy converters as shown in Eq. (1);

$$P = \frac{1}{2} C_P \rho A V^3 \tag{1}$$

where C_P is the turbine power coefficient which typically lies between 0.2 and 0.4. V is the velocity, ρ is the water density, and A is the swept area of the rotor.

Double-multiple Stream Tube Model (DMST). is based on the calculation of flow velocity through the turbine by equating the stream-wise hydrodynamics force imparted on the blades with the rate of change of momentum. The key future of DMST is dividing the turbine swept area into two parts as upstream half-cycle of the rotor and downstream half-cycle of the rotor. Throughout this paper, the term 'up' will refer to the upwind half cycle and 'dn' for the downwind half cycle. DMST model is capable of calculating the difference in the induced velocities at the upstream (V_{up}) and downstream (V_{dn}). V_{up} and V_{dn} at each level of the rotor were obtained using the principle of two actuator disks (an ideal model used to represent the rotor as an infinitely thin disk) in tandem as illustrated in Fig. 1. Then by averaging the contribution of each stream- tubes the torque, power, lift, and drag can be calculated. In the DMST model the upcoming free stream velocity, V_∞, is reduced by interference factors of a_{up} in the upstream and a_{dn} in the downstream. The axial induction factors proceed by discretization of each disk into multiple stream tube models. Azimuthal discretization of stream tubes is the first step in DMST, each stream-tubes located by the Azimuthal angle as shown in Fig. 2. For simplicity, it can be considered that each stream tubes are parallel to each other and each stream tube can be assumed as independent of each other. The area occupied by each stream-tube A_i can be calculated by discretization the azimuthal angle to infinitesimal $\delta\theta$ as shown in Fig. 2.

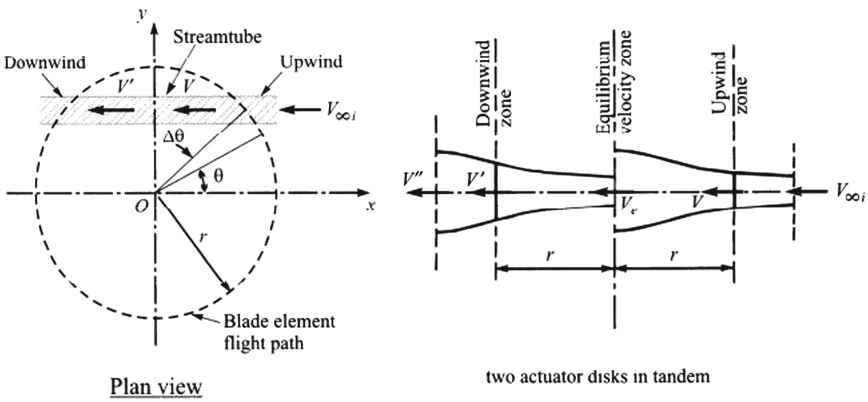

Fig. 1. Double multi stream-tube model diagram [15]

$$A_i = (R\delta\theta)(\delta h sin\theta_i) \tag{2}$$

Hence, the induced V_{up}, at equilibrium, V_e, and V_{dn} is calculated using;

$$V_{up} = a_{up}V_\infty \tag{3}$$

$$V_e = (2a_{up} - 1)V_\infty \tag{4}$$

$$V_{dn} = a_{dn}(2a_{up} - 1)V_\infty \tag{5}$$

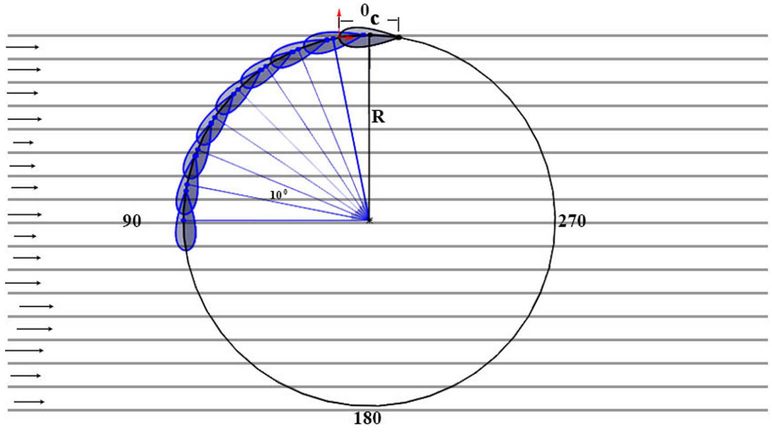

Fig. 2. Azimuthal discretization of stream tubes (shown in the straight lines), the azimuthal location of the blade is shown in the figure at every 10^0 for $0 \leq \theta \leq 90$

The remaining part of this section will present the DMST mathematical formulation for the upwind half cycle, the same procedure can be performed for the downstream half cycle only by replacing V_{up} by V_{dn}. The velocity diagram for DMST is expressed in Fig. 3 considering the pitch angle as zero. Then the local angle of attack can be calculated using the following equation,

$$\alpha = tan^{-1}\left(\frac{V_{up}sin\theta_i}{V_{up}cos\theta_i + \omega R}\right) \tag{6}$$

where TSR is calculated as $TSR = (\omega R)/V_{\infty}$, similar the relative velocity is expressed as follows;

$$w = \sqrt{(V_{up}cos\theta_i + \omega R)^2 + (V_{up}sin\theta_i)^2} \tag{7}$$

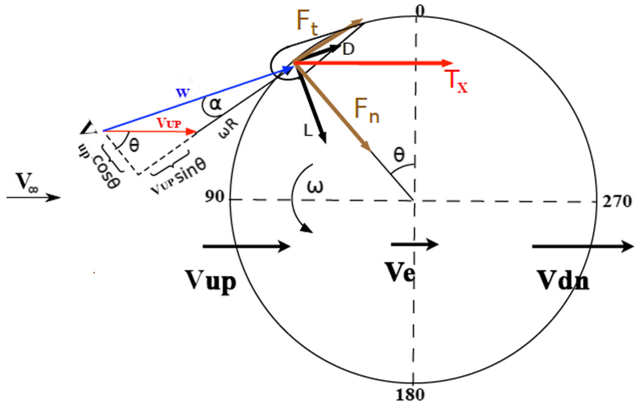

Fig. 3. Velocity triangle diagram and Force components [3]

The Reynolds number then can be computed as

$$Re = \frac{cw}{\nu} \tag{8}$$

After the velocity diagram is resolved the next step is to calculate the force components which are shown in Fig. 3. The normal force F_n and tangential force F_t can be expressed by the force coefficients for each as;

$$C_N = C_L cos\alpha + C_D sin\alpha \tag{9}$$

$$C_T = C_L sin\alpha - C_D cos\alpha \tag{10}$$

Then

$$F_n = \frac{1}{2} w^2 c\delta h C_N \tag{11}$$

$$F_t = \frac{1}{2} w^2 c\delta h C_T \tag{12}$$

The total effect of F_t and F_n on hydrofoil will create an axial force F_X, for one turbine blade it can be found by decomposing in the axial direction as

$$F_X = F_N sin\theta_i - F_T cos\theta_i \tag{13}$$

for N number of blades the total axial force will be

$$\overline{F_X} = N \frac{\delta\theta}{2\pi} F_X \tag{14}$$

Then the axial thrust coefficient computed as;

$$C_X = \frac{\overline{F_X}}{\frac{1}{2}\rho V_\infty^2 A} = \frac{Nc}{2\pi R} \frac{w^2}{V_\infty^2} \frac{1}{|\sin\theta_i|} (C_N \sin\theta_i - C_T \cos\theta_i) \tag{15}$$

The axial trust coefficient then computed with the momentum theory to solve the iteration scheme of DMST to find a_{up}

$$4a_{up}(1 - a_{up}) = C_X = \frac{\overline{F_X}}{\frac{1}{2}\rho V_\infty^2 A} = \frac{Nc}{2\pi R} \frac{w^2}{V_\infty^2} \frac{1}{|\sin\theta_i|} (C_N \sin\theta_i - C_T \cos\theta_i) \tag{16}$$

The calculations at downstream, as repeated previously, can be performed in a identical manner to those of the upstream by considering the following modification of the stream velocity as

$$V_{dn} = (1 - a_{up}) V_e = (1 - a_{dn}) (1 - 2a_{up}) V_\infty \tag{17}$$

$$C_X^{dn} = 4a_{dn} (1 - a_{dn}) (1 - 2a_{up})^2 \tag{18}$$

The torque, power, and power coefficient then can be determined as

$$T_i = \frac{1}{2}\rho W_{\infty,i}^2 c\Delta h C_{T,i} * R \tag{19}$$

$$T_{tot} = N_P \left[\frac{1}{2N_\theta} \left(\sum_{k=1}^{N_\theta} T_i^{up} + \sum_{k=1}^{N_\theta} T_i^{dn} \right) \right] \tag{20}$$

$$P = \Omega T_{tot} \tag{21}$$

$$C_P = \frac{P}{\frac{1}{2}\rho V_0^3 A} \tag{22}$$

2.2 Analytical Performance Predication of Vertical-Axis Hydrokinetic Turbines

To predict the performance of VAHKTs the process started by specifying the turbine geometric and working condition parameters. The design flow is shown in Fig. 4, to implement the design procedure a NACA 0021 hydrofoil was used. We refer to the design guideline proposed by [5] for optimizing the annual energy yield.

Using the flow chart shown in Fig. 4 a design specification parameter were developed for the performance prediction as shown in Table 1. The required water velocity data was referred from the work of [21], and the experimental result of the hydrofoil data for NACA 0021 was taken from the [18]. However, the data provided by the [18] only contain the range of $0 < \alpha < 180$ and limited Re. Hence, a panel method using an XFoil is available at https://web.mit.edu/drela/Public/web/xfoil/ to generate the hydrofoil data of the rang of $-20 \leq \alpha \leq 20$ for different Re of 50,000, 100,000, 200,000, 500,000, and 1,000,000 was used. For the other range of α the influence of Re is limited to the region of low α, Hence experimental data of [18] were used. Using the experimental result of [18] the relation for C_l and C_D above $\alpha > 20\,\&\&\,\alpha < -20$ a polynomial fit

Table 1. Geometric and working condition specification of VAHKTs

Parameters	Value
Radius of the rotor (m)	0.125
Diameter of the rotor (m)	0.25
Height of the blade (m)	0.4
Number of blades	3
Chord length (m) of the hydrofoil	0.03
Type of hydrofoil	NACA0021
Operating Reynolds number	50,000, 100,000, 200,000, 500,000, and 1,000,000
Kinematic viscosity of water at 20 °C (m^2/s)	1.004e − 6
Incoming velocity range (m/s)	0.75, 1.5, 2, 2.5, and 3

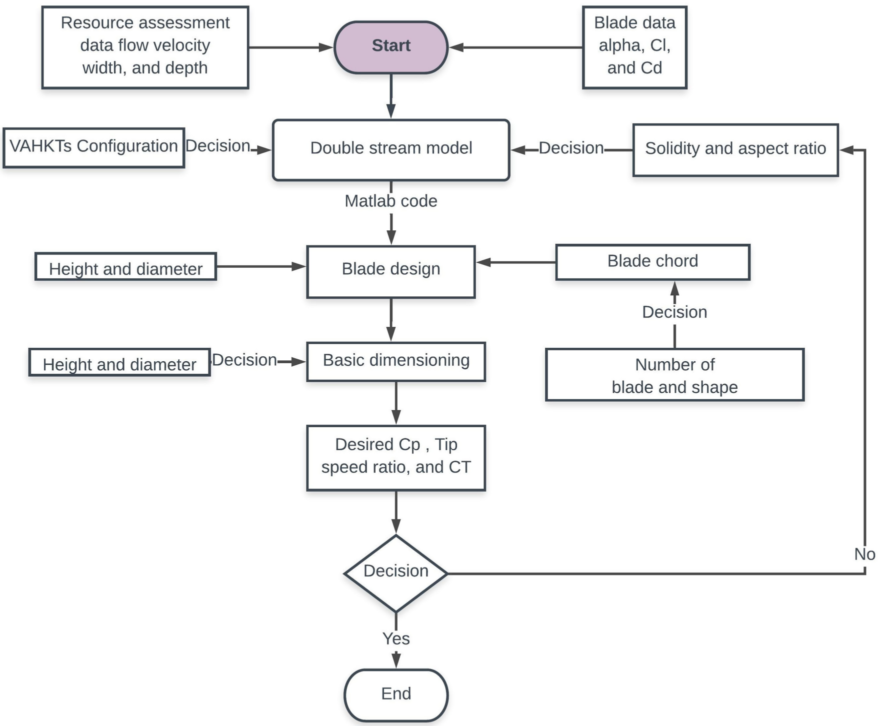

Fig. 4. Design flow chart for H-VAHKTs

were generated using a MATLAB cure fitting tool with the 4^{th} order with the $R^2 = 0.9817$ at Coefficients with 95% confidence bounds and express as follows.

$$C_l = -1.232 \times 10^{-8}\alpha^4 + 8.605 \times 10^{-6}\alpha^3 - 0.0017\alpha^2 + 0.1047\alpha - 0.9 \quad (23)$$

$$C_D = 2.178 \times 10^{-8}\alpha^4 - 7.569 \times 10^{-6}\alpha^3 + 0.00056\alpha^2 + 0.01912\alpha - 0.3 \quad (24)$$

To predict the performance, equations presented in Sect. 2.1 were used to develop a Matlab code. The general Proceeder used to solve the DMST using a Matlab code is given as;

1. The analytical simulation using the DMST model begins by specifying the geometries and working conditions of VAHKTs a seen from Table 1.
2. Then the discretization of the rotor into 36 stream tubes was followed i.e. 18 stream tubes for each up and downstream of the rotor and the azimuthal discretization is performed for every 10^0.
3. The iterations initiated for the upstream section by a wild guess of $a_{up} = 1$.
4. Then the angle of attack, relative velocity, and Reynolds number calculated using Eq. (6), (7), and (8) respectively.

5. Using the Panel data of Xfoil and experimental data of [18] the C_l and C_D at different α were used to estimate the required C_D and C_N, Eq. (9) and (10) used.
6. The required hydrodynamics forces then calculated using Eqs. (11), (12), and (13).
7. Then the first induction factor is estimated using Eq. (16), then the iteration continues until the difference between the induction factors is $< 10^{-6}$.
8. Once the value of induction factor in desired range C_P is calculated for the up-stream of half the rotor using Eq. (22).
9. Then the same procedure is repeated for the other half of the downstream rotor by replacing the velocity relation given in Eq. (3), (4), and (5).
10. Finally the C_P for both half of the rotor will be added to get the total C_P.

2.3 Experimental Setup and Validation

The primary objective of the experimental work is to validate the results of DMST model performance prediction. The experiment was conducted based on a water loop flume of S6-MKII. S6-MKII flume is assembled from a modular section of 2 m length and 300 mm wide by 450 mm deep cross-section as shown in the schematic of Fig. 5. The experimental work is carried for a velocity of 1.2 m/s.

We developed the prototype of the VAHKT based on the specifications provided in Table 1, it is made with a thermoplastic polymer Polylactic Acid (PLA) material using a 3D printer. The 3D model and the developed prototype is as shown in Fig. 6.

The instruments used for measurements were a Valeport BFM002 S-N 2065 current meter to measure the velocity, a tachometer, to measure the angular velocity ω, and a load cell-based torque measurement, to measure T, as shown in Fig. 7.

The procedure we followed to conduct the experiment started by first placing the turbine's unit assembly in the test rig of the S6-MKII flume, then the experiment was started by measuring the upstream velocity using the current meter and then a 5 min. time has given the turbine to be in the fully developed rotation and ω was measured then we the torque measurements were carried out. The available C_P was calculated using the fowling equation;

$$C_P = \frac{T\omega}{1/2\rho A V^3} \tag{25}$$

To further validate both the experimental and DMST results we used also the experimental result of a reference model (RM2) developed by U.S. Department of Energy's (DOE) [10] the for validation, the specification of RM2 is given in Table 2.

Fig. 5. S6-MKII Test rig flume, the section shown in red is the location of the test. (Color figure online)

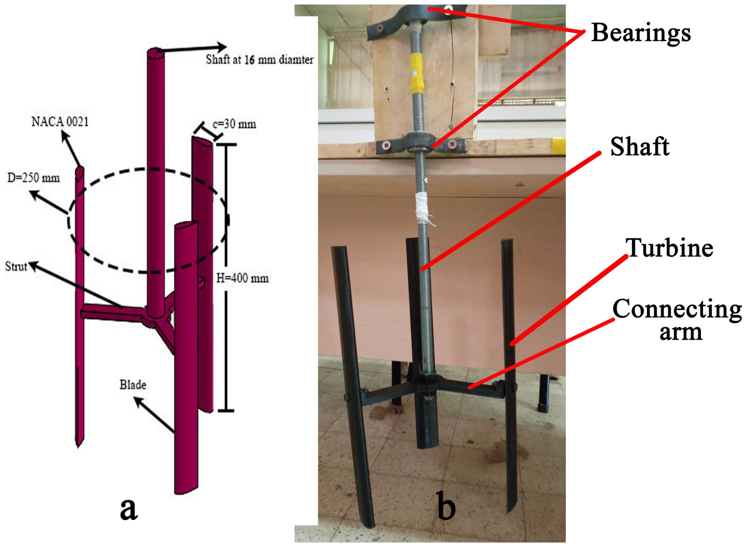

Fig. 6. (a) 3D model of the VAHKTS and (b) prototype used for the test

3 Results and Discussion

3.1 DMST Performance Evaluation

We developed a Matlab code to predict the performance of VAHKTs under different water velocities of 0.75, 1.5, 2, 2.5, and 3 m/s for each V_∞ we solve for

Fig. 7. Measuring instruments

Table 2. Specification of RM2 reference turbine

Parameter	RM2 turbine geometries
Blade Profile	NACA 0021
Max Blade Chord Length	0.0267 m
Rotor Height	0.323 m
Rotor Diameter	0.43 m
Rotor Shaft Diameter	0.0254 m
Solidity	0.047
Tip-Speed Ratios	1 to 4

different tip speed ratio of 1, 2, 3, 4) and C_P is predicted. For each case 1000 iterations were carried out, the convergence criteria are set to bellow 10^{-6}.

It is evident from Fig. 8 the maximum operating condition with high performance C_P is when the V_∞ is 2.5 m/s and at 2.5 TSR. DMST also provides insightful velocity distributions across the azimuthal location of the turbine. For example, referring to Fig. 9 the reduction of V_∞ by the turbine in the upwind and downwind of the rotor can be demonstrated when V_∞ of 1.5 m/s and 2.5 m/s and at 3 TSR. Figure 10 showed the contribution of each blade to the generation of torque, it can be shown that the first power starts produced by the first blade and then the second blade while blade three produces net zero positive torque.

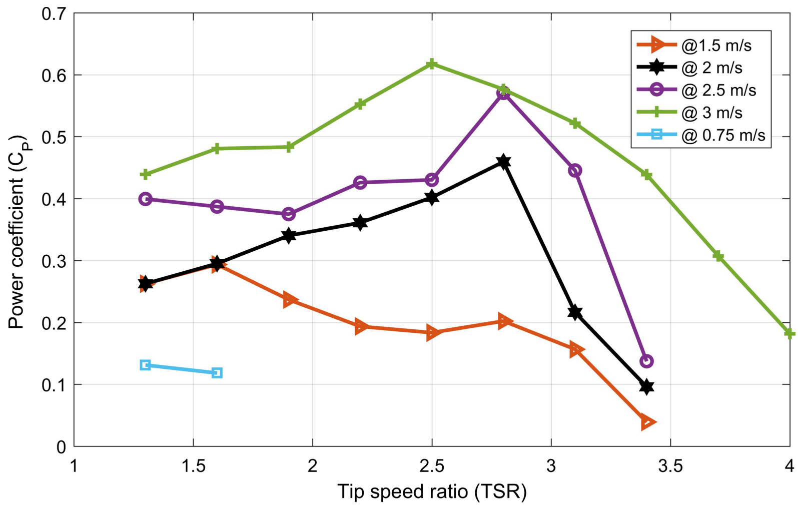

Fig. 8. DMST performance prediction of VAHKTS under different v_∞

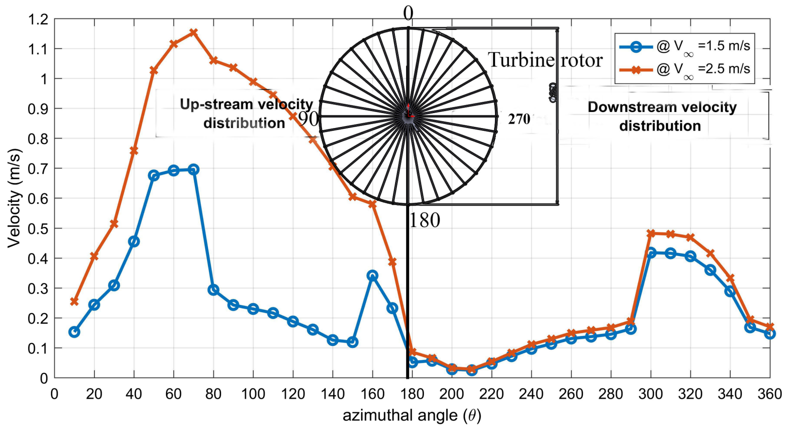

Fig. 9. Velocity distribution in the half up and down stream of the rotor.

3.2 Experimental Performance Evaluation

The experimental investigation were carried out to validate the DMST results at the V_∞ of 1.2 m/s, the TSR is calculated as $TSR = (\omega R)/V_\infty$. The result from measurement is summarized in the following Table 3.

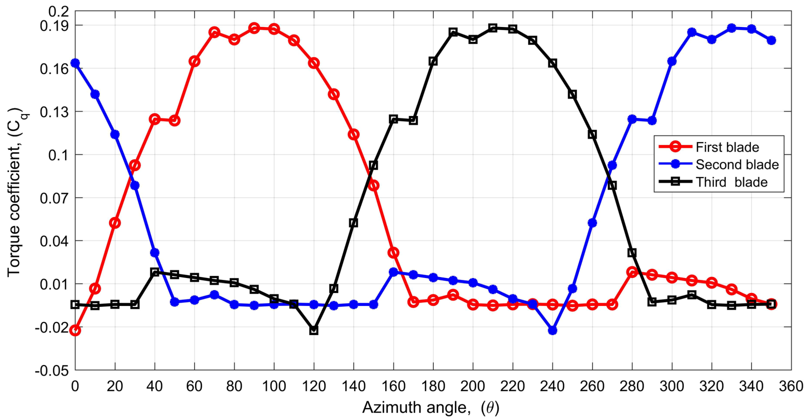

Fig. 10. Torque coefficient performance of single blade at different azimuthal angle

Table 3. Experimental results

	Measurements		TSR	C_P
	Torque (Nm)	ω (RPM)		
$V_\infty = 1.2\,\mathrm{m/s}$	0.051	95	1.03	0.0115

3.3 Compression of DMST and Experimental Performance with Reference Turbine

Performance studies of RM2 reference turbine were carried out in a large open channel facility where the volumetric flow rate, $Q = 2.35\,\mathrm{m}^3/s$, the velocity of $V_\infty = 1.2\,\mathrm{m/s}$, and with $Re = 6.1\times10^4$. From the performance test at $TSR = 2.2$ Optimal performance occurred with $C_P = 0.07$. The comparison made between the DMST, experimental, and RM2 reference model, which is shown in Table 4;

Table 4. Compression of DMST and experimental performance with reference turbine, at $V_\infty = 1.2\,\mathrm{m/s}$

TSR	DMST	Experiment	RM2
1.10	0.098	0.0115	0.007
1.33	0.165	–	0.017
1.55	0.2449	–	0.029
2.20	0.18	–	0.070
2.90	−0.0636	–	−0.05

From Table 4 C_P were over predicted by DMST, while the experimental and RM2 result showed a good agreement.

4 Conclusions

The purpose of the current study was to predict the performance of VAHKTs through DMST and experimental study. The Performance investigation using DMST was carried out for different water velocities. The DMST model showed that higher C_P is observed when TSR is 2.5 and the upcoming upstream velocity is 3 m/s. To validate the DMST model experimental studies were carried out, the experiments confirmed the Result obtained from DMST. Further compression is made by RM2 with the DMST and experimental which showed good consistency. The simulation tools are therefore useful for designing vertical axis turbines.

References

1. Anyi, M., Kirke, B.: Evaluation of small axial flow hydrokinetic turbines for remote communities. Energy Sustain. Dev. **14**(2), 110–116 (2010). https://doi.org/10.1016/j.esd.2010.02.003. https://www.sciencedirect.com/science/article/pii/S0973082610000128
2. International Hydropower Association: 2020 Hydropower Status Report — International Hydropower Association (2020). https://archive.hydropower.org/publications/2020-hydropower-status-report
3. Ayati, A.A., Steiros, K., Miller, M.A., Duvvuri, S., Hultmark, M.: A double-multiple streamtube model for vertical axis wind turbines of arbitrary rotor loading. Wind Energy Sci. **4**(4), 653–662 (2019). https://doi.org/10.5194/wes-4-653-2019. https://wes.copernicus.org/articles/4/653/2019/
4. Bangga, G., Dessoky, A., Lutz, T., Krämer, E.: Improved double-multiple-streamtube approach for H-Darrieus vertical axis wind turbine computations. Energy **182**, 673–688 (2019). https://doi.org/10.1016/j.energy.2019.06.083. https://www.sciencedirect.com/science/article/pii/S0360544219312149
5. Bianchini, A., Ferrara, G., Ferrari, L.: Design guidelines for H-Darrieus wind turbines: optimization of the annual energy yield. Energy Convers. Manag. **89**, 690–707 (2015). https://doi.org/10.1016/j.enconman.2014.10.038. https://www.sciencedirect.com/science/article/pii/S0196890414009194
6. Chica, E., Pérez, F., Rubio-Clemente, A., Agudelo, S.: Design of a hydrokinetic turbine, Medellin, Colombia, pp. 137–148, September 2015. https://doi.org/10.2495/ESUS150121. http://library.witpress.com/viewpaper.asp?pcode=ESUS15-012-1
7. Dai, Y.M., Gardiner, N., Sutton, R., Dyson, P.K.: Hydrodynamic analysis models for the design of Darrieus-type vertical-axis marine current turbines. Proc. Inst. Mech. Eng. Part M J. Eng. Marit. Environ. **225**(3), 295–307 (2011). https://doi.org/10.1177/1475090211400684. https://doi.org/10.1177/1475090211400684
8. Goude, A.: Fluid Mechanics of Vertical Axis Turbines: Simulations and Model Development. Ph.D. thesis, Uppsala University, Electricity (2012)
9. Güney, M., Kaygusuz, K.: Hydrokinetic energy conversion systems: a technology status review. Renew. Sustain. Energy Rev. **14**(9), 2996–3004 (2010). https://doi.org/10.1016/j.rser.2010.06.016. https://www.sciencedirect.com/science/article/pii/S1364032110001632

10. Hill, C., Neary, V.S., Gunawan, B., Guala, M., Sotiropoulos, F.: U.S. department of energy reference model program RM2: experimental results. https://doi.org/10.2172/1171458. https://www.osti.gov/biblio/1171458
11. Islam, M., Ting, D.S.K., Fartaj, A.: Aerodynamic models for Darrieus-type straight-bladed vertical axis wind turbines. Renew. Sustain. Energy Rev. **12**(4), 1087–1109 (2008). https://doi.org/10.1016/j.rser.2006.10.023. https://www.sciencedirect.com/science/article/pii/S136403210600164X
12. Khan, M., Iqbal, M., Quaicoe, J.: Design considerations of a straight bladed Darrieus rotor for river current turbines. https://doi.org/10.1109/ISIE.2006.295835
13. Khan, M., Iqbal, M., Quaicoe, J.: River current energy conversion systems: progress, prospects and challenges. Renew. Sustain. Energy Rev. **12**(8), 2177–2193 (2008). https://doi.org/10.1016/j.rser.2007.04.016. https://www.sciencedirect.com/science/article/pii/S136403210700069X
14. Moghimi, M., Motawej, H.: Developed DMST model for performance analysis and parametric evaluation of Gorlov vertical axis wind turbines. Sustain. Energy Technol. Assess. **37**, 100616 (2020). https://doi.org/10.1016/j.seta.2019.100616. https://www.sciencedirect.com/science/article/pii/S2213138819306691
15. Paraschivoiu, I.: Wind Turbine Design: with Emphasis on Darrieus Concept. Polytechnic International Press (2002). https://books.google.com.et/books?id=sefVtnVgso0C
16. Paraschivoiu, I.: Double-multiple streamtube model for studying vertical-axis wind turbines. J. Propul. Power **4**(4), 370–377 (1988). https://doi.org/10.2514/3.23076
17. Roh, S.C., Kang, S.H.: Effects of a blade profile, the Reynolds number, and the solidity on the performance of a straight bladed vertical axis wind turbine. J. Mech. Sci. Technol. **27**(11), 3299–3307 (2013)
18. Sheldahl, R.E., Klimas, P.C.: Aerodynamic characteristics of seven symmetrical airfoil sections through 180-degree angle of attack for use in aerodynamic analysis of vertical axis wind turbines. https://doi.org/10.2172/6548367. https://www.osti.gov/biblio/6548367
19. Soukhaphon, A., Baird, I.G., Hogan, Z.S.: The impacts of hydropower dams in the Mekong river basin: a review. Water **13**(3), 265 (2021). https://www.mdpi.com/2073-4441/13/3/265
20. Sovacool, B.K., Walter, G.: Internationalizing the political economy of hydroelectricity: security, development and sustainability in hydropower states. Rev. Int. Polit. Econ. **26**(1), 49–79 (2019). https://doi.org/10.1080/09692290.2018.1511449
21. Tigabu, M.T., Wood, D., Admasu, B.T.: Resource assessment for hydro-kinetic turbines in Ethiopian rivers and irrigation canals. Energy Sustain. Dev. **58**, 209–224 (2020). https://doi.org/10.1016/j.esd.2020.08.005. https://www.sciencedirect.com/science/article/pii/S0973082620302866
22. VanZwieten, J., et al.: In-stream hydrokinetic power: review and appraisal. J. Energy Eng. **141**(3), 04014024 (2015). https://doi.org/10.1061/(ASCE)EY.1943-7897.0000197
23. Vermaak, H.J., Kusakana, K., Koko, S.P.: Status of micro-hydrokinetic river technology in rural applications: a review of literature. Renew. Sustain. Energy Rev. **29**, 625–633 (2014). https://doi.org/10.1016/j.rser.2013.08.066. https://www.sciencedirect.com/science/article/pii/S1364032113006060
24. Wu, Y.K., Lin, H.J., Lin, J.H.: Certification and testing technology for small vertical axis wind turbine in Taiwan. Sustain. Energy Technol. Assess. **31**, 34–42 (2019). https://doi.org/10.1016/j.seta.2018.11.005. https://www.sciencedirect.com/science/article/pii/S2213138817300279

25. Zarfl, C., Lumsdon, A.E., Berlekamp, J., Tydecks, L., Tockner, K.: A global boom in hydropower dam construction. Aquat. Sci. **77**(1), 161–170 (2015). https://doi.org/10.1007/s00027-014-0377-0
26. Zeiner-Gundersen, D.H.: A vertical axis hydrodynamic turbine with flexible foils, passive pitching, and low tip speed ratio achieves near constant RPM. Energy **77**, 297–304 (2014). https://doi.org/10.1016/j.energy.2014.08.008. https://www.sciencedirect.com/science/article/pii/S036054421400944X